Mem. S.A.It. Vol. 81, 414
© SAIt 2010
Memorie della

A multi-wavelength view of M81*

M. Nowak[1], S. Markoff[2], and A. Young[3]

[1] Kavli Institute for Astrophysics and Space Research, Massachusetts Insitute of Technology, 77 Massachusetts Ave., Cambridge, MA 02139
e-mail: `mnowak@space.mit.edu`
[2] Astronomical Institute "Anton Pannekoek" University of Amsterdam Kruislaan 403 1098 SJ Amsterdam, The Netherlands
[3] H.H. Wills Physics Laboratory, University of Bristol, Tyndall Avenue, Bristol BS8 1TL, UK

Abstract. Our group has used the High Energy Transmission Gratings (HETG) on board the Chandra X-ray telescope to perform deep, high-resolution spectroscopic observations of the Low Luminosity Active Galactic Nuclei (LLAGN) M81*. Along with these X-ray spectroscopic observations, we performed a series of simultaneous and near simultaneous radio observations. M81* is of particular interest because of its low fractional Eddington luminosity. It may represent an Advection Dominated Accretion Flow. Thus we discuss models where the emission is from a hot, inflowing plasma. It is also of interest because of its radio emission from a jet, which in some ways is similar to the even lower luminosity Galactic Center source, Sgr A*. It has been hypothesized the the class of LLAGN represent a stage of accretion flow onto black holes wherein the emission is dominated by the jet flow. We thus present jet-models of M81*.

1. Introduction

M81*, the central X-ray source in the nearby spiral galaxy M81, is the closest *unobscured* Active Galactic Nucleus (AGN). Even though it is an intrinsically faint source, owing to its proximity we have a good knowledge of its basic properties. It lies at a distance of 3.64 ± 0.34 Mpc (Freedman et al. 1994) and has a likely mass of $7 \pm 2 \times 10^7\ M_\odot$ (Devereux et al. 2003). However, it has a low luminosity of only $\approx 10^{-5}\ L_{\rm Edd}$. Thus, it belongs to the class of Low Luminosity Active Galactic Nuclei (LLAGN) (similar, for example, to the maser galaxy, NGC 4258; Makishima et al. 1994).

These class of sources are interesting for several reasons. First, they are to be contrasted with normal Seyfert 1 galaxies, which tend to lie at luminosities $> 1\%\ L_{\rm Edd}$. In contrast to such sources, however, LLAGN show stronger radio flux compared to their X-ray flux. This might be similar to "hard state" galactic black hole candidate (GBHC) sources which become radio-loud (and X-ray spectrally hard) at fluxes $< 1\%\ L_{\rm Edd}$. It has been suggested that at such low fluxes (and hard X-ray spectra) that both AGN and GBHC enter a regime of jet-dominated emission in the *radio through the X-ray bands* (Falcke et al. 2004).

Second, it has been suggested that such low accretion rates might represent a regime of Advection Dominated Accretion Flows

Send offprint requests to: M. Nowak

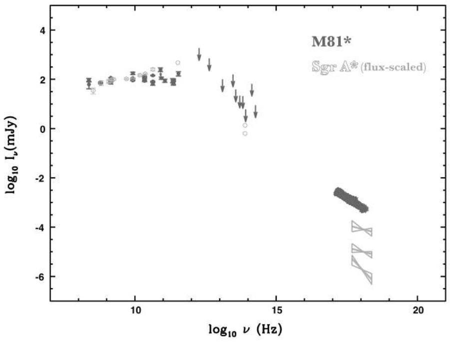

Fig. 1. Comparison between the multi-wavelength spectrum of M81* (see Fig. 5) and Sgr A* (see Markoff et al. 2008). The spectrum of Sgr A* has been scaled so that its radio flux matches that of M81*. Only during X-ray flares (see Baganoff et al. 2001) does the ratio of X-ray to radio flux in Sgr A* approach that of M81*. Sgr A*, however, is at a much lower fractional Eddington luminosity. Note that the upper IR/optical upper limits shown in the figure come from non-simultaneous HST, ISO, and MIRLIN measurements (Grossan et al. 2001; Gordon et al. 2004; Murphy et al. 2006).

(ADAFs) (Narayan & Yi 1995), or Radiatively Inefficient Accretion Flows (RIAF). In such flows rather than the energy liberated by accretion being radiatively lost, it is instead advected through the event horizon of the black hole, and/or lost as thermal energy in an outward flowing wind.

The other well-studied source suggested to be jet-dominated and radiatively inefficient is our own Galactic Center, Sgr A*. Indeed, M81* shows spectral similarities to Sgr A* (see Fig. 1). The ratio of X-ray flux to radio flux, however, is relatively weaker in Sgr A*, except during its X-ray flares. Although closer, Sgr A* is even *more* sub-Eddington than M81*, and is behind a larger column of material, and thus is unsuited for high resolution X-ray spectroscopic study. We thus embarked upon a program to study the detailed X-ray and radio spectra of M81*.

2. Chandra-HETG observations

In 2005 we conducted a 300 ksec observing program using the Chandra-High Energy Transmission Gratings (HETG). With a bandpass of 0.4–8 keV and a spectral resolution of $E/\Delta E$ up to 1000, HETG is well-suited for detailed X-ray spectroscopy, including plasma diagnostics, of astrophysical sources. As discussed by Young et al. (2007), we indeed discovered line emission from M81* – the first detection of such X-ray spectroscopic lines from an LLAGN. Here we present new figures of these data that incorporate an additional 150 ksec from a campaign conducted a year later (PI: J. Miller). None of the basic conclusion of Young et al. (2007) are changed; however, the signal-to-noise has been improved.

The overall spectrum is shown in Fig. 2. Here we fit a simple phenomenological model, without any line emission, and show the residuals to highlight the line features. What is immediately obvious is that we see emission features from material at a *variety* of temperatures. Cold material is highlighted by the presence of both Si and Fe Kα fluorescence features (Fig. 3). Warm material (10^6–10^8 K) is highlighted by the presence of emission from various ionized species (O VIII, Ne X, Si XIII, Si XIV; Fig. 2 and 3). Hot material ($> 10^{7.4}$ K) is highlighted by the presence of emission from highly ionized species, namely Fe XXV and Fe XXVI.

As discussed by Young et al. (2007), several things can be learned from detailed fitting of these lines. First, looking at the He-like triplet of Si XIII, we note that the "G ratio" of the line strength of (forbidden+intercombination) to resonance line is $0.6^{+0.9}_{-0.2}$. This is consistent with a collisionally ionized plasma, as opposed to a photoionized plasma. Additionally, a number of the lines show velocity widths $> 500\,\mathrm{km\,s^{-1}}$, with the Fe XXV and Fe XXVI lines showing velocity widths approaching $2000\,\mathrm{km\,s^{-1}}$. The latter two lines are also redshifted by comparable amounts.

Thus, these lines must originate within $\approx 10^4\ GM/c^2$ of the black hole. They are consistent with hot, flowing material as one might expect from a RIAF. Young et al. (2007) con-

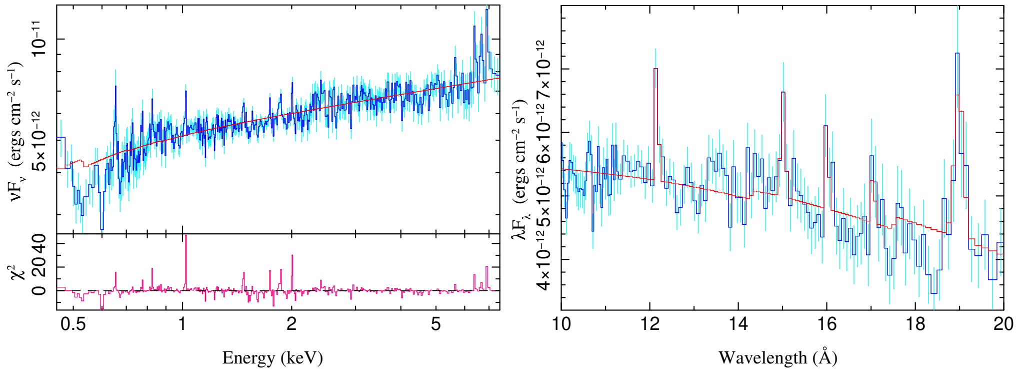

Fig. 2. Left: The summed data from our $\approx$ 300 ksec HETG-campaign (Young et al. 2007; Markoff et al. 2008),plus an additional 150 ksec from a recent monitoring campaign (PI: J. Miller). The spectrum has been fit with a simple model consisting of galactic absorption, a soft excess, and a power law. The residuals show emission lines from material with a likely range of temperatures of $\approx 10^6$–10^8 K. Right: A close-up view of the O-edge region with gaussian lines added to the fit. Detected emission lines include: Oviii Kα and Kβ, Fexvii (15, 17 Å), and Nex.

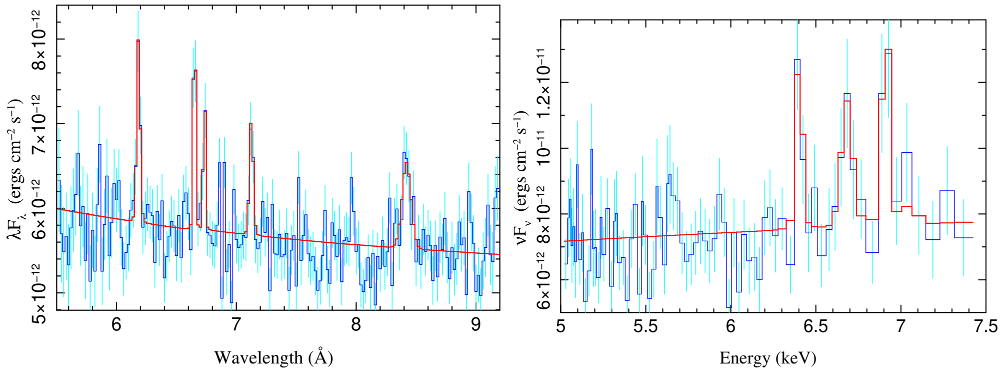

Fig. 3. Left: The 5.5–9 Å region fit with emission lines of Si and Mg. Visible are Si Kα, Sixiv, Sixiii, and Mg xii. The Sixiii He-like triplet only shows emission from the resonance and forbidden lines – the intercombination line is weak or absent (Young et al. 2007). Right: The Fe line region with fitted emission lines for Fe Kα, Fexxv and Fexxvi. The latter two lines are redshifted and broadened by $\approx$ 2000 km s^{-1}, indicating that the emission arises within $\approx 10^4\ GM/c^2$ (Young et al. 2007).

ducted an "emission measure" analysis, and in fact showed that one can explain the lines and their velocity widths with an inflowing plasma with temperatures ranging from $\approx 10^6$–10^9 K within radii $< 10^4\ GM/c^2$. This further can account for $\approx 75\%$ of the continuum; however, 25% must come from an additional, power-law like source.

3. Multi-wavelength campaign

The collisional plasma model described above, however, leaves unexplained the radio emission, and provides for no coupling between the radio and X-ray emission. To explore the possibility of such coupling, we arranged for all of our Chandra-HETG observations to be si-

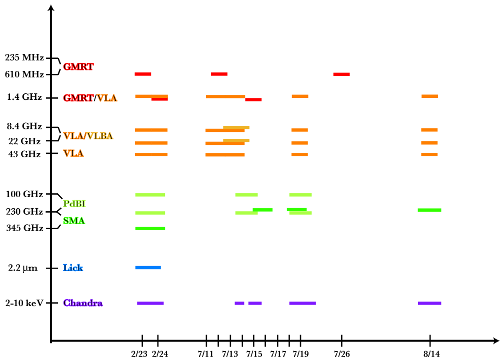

Fig. 4. Schematic overview of the multi-wavelength coverage over the course of the entire 2005 campaign to observe M81*. The Chandra observations all occurred at roughly comparable 0.8-8 keV fluxes. For details of coverage on individual days, see Markoff et al. (2008).

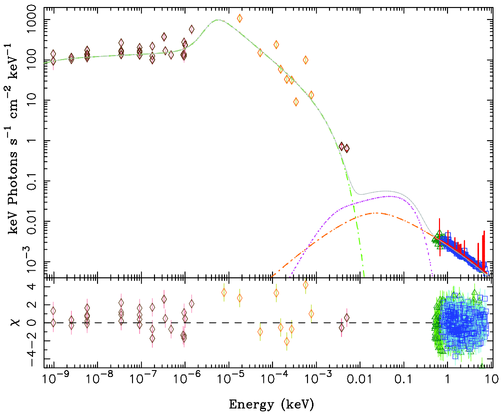

Fig. 5. An example fit to the multi-wavelength data of M81* using the jet model (Markoff et al. 2008). Note that here we are using the IR/optical limits from Spitzer, ISO, HST, and MIRLIN as fit-data.

multaneous with radio observations from multiple observatories. A schematic of this multi-wavelength campaign is shown in Fig. 4. This work is described in full detail in Markoff et al. (2008).

We fit all of these data, both collectively and on an individual observation basis, with the jet-model described by Markoff et al. (2001). There are four basic assumptions in the model: 1) the total power in the jets scales with the total accretion power at the innermost part of the accretion disk, $\dot{M}c^2$, 2) the jets are freely expanding and only weakly accelerated via their own internal pressure gradients, 3) the jets contain cold protons which carry most of the kinetic energy, while leptons dominate the radiation, and 4) some or all of the originally thermally distributed particles are accelerated into a power-law which is maintained along the rest of the jet via distributed acceleration.

The basic emission components of this model are synchrotron emission from the pre- and post-acceleration zones of the jet, synchrotron self-Compton, disk emission from cold material close to the black hole, and Comptonization of disk emission. As shown in Fig. 5, this model does an excellent job of reproducing the observed properties of the mutli-wavelength emission. It should also be emphasized that Fig. 5 represents an actual fit, i.e., the spectral model has been folded through the response of Chandra-HETG, and simultaneously fitted to the radio.

Furthermore, the jet parameters that we find are comparable to those derived from spectral fits to low/hard state GBHC spectra. Specifically, fits to Cyg X-1 (Markoff et al. 2005) show comparable parameters, albeit with a higher power in the jet (relative to the Eddington luminosity) than is required for M81*.

4. Conclusions

The simultaneous radio/Chandra-HETG campaign discussed by Young et al. (2007) and Markoff et al. (2008) provided us with our first glimpses into the detailed workings of an LLAGN. Clear evidence was found for the existence of hot, line emitting plasma in the central regions of the system, i.e., at radii $< 10^5\ GM/c^2$. This could be consistent with models of Advection Dominated Accretion Flows. Furthermore, we found that jet models also provide a very good description of both the radio and X-ray spectra.

M81* is perhaps the prime example of a system for which the proposed International X-ray Observatory (IXO) will be capable of making major contributions. With significantly more effective area than the Chandra-HETG (or even XMM-Newton CCDs), and with greater spectral resolution than the gratings, IXO will be able to quickly obtain a detailed spectrum of M81*, and over multiple observations, be able to follow the correlation of the line properties with the continuum.

Specifically, a 50 ksec IXO observation would have the same signal-to-noise per bin as the 450 ksec observation shown in Fig. 2; however, that will be achieved with > 6 times the number of resolution elements. Thus, a straw man 450 ksec IXO program to observe M81* might consist of 9×50 ksec observations, each yielding more than 6 times the resolution shown in the figures here, capable of tracking detailed line properties vs. spectral flux.

As shown in Fig. 6, M81* can show large flux changes over the course of such a campaign. (The observations discussed here span less than two years.) Note also there is some evidence already for line variability over this period. (Note that the lowest flux summed observation has a higher Ne X flux than the next higher flux summed observation.) Such line variability would place even more stringent constraints on the location of the line emitting accretion flow (i.e., placing it closer to the central compact object).

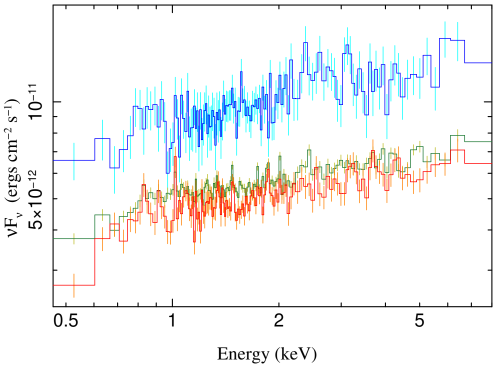

Fig. 6. All the individual Chandra-HETG observations of M81* summed together into three spectra. The lower two spectra contain nearly half each of the observational time, and represent the flux range observed within our initial radio/Chandra campaign. The highest flux spectrum comes from two, recent Chandra-HETG observations (Miller et al. 2009, in prep.), and are a combined 30 ksec. From these observations we see that M81* is capable of at least a factor of 3 variability in the 0.8–8 keV band.

5. DISCUSSION

ANDRZEJ ZDZIARSKI: When you fit the jet model to spectra of Cyg X-1 (i.e., Markoff et al. 2005), you required a fine tuning of the parameters to fit the high energy rollover in the hard tail with Comptonization, and you had a very high coronal temperature. Here for your fits of M81* the temperatures of your corona are also very high, and your corona are very optically thin.

MICHAEL NOWAK: There are two separate, but related issues here: the "fine tuning" of the jet model parameters to fit the exponential rollover at high energies, and the temperature of the corona itself. For the first point, I note that if you look at fits to "hard state" spectra of Cyg X-1 (Wilms et al. 2006) and GX 339−4 (Nowak et al. 2005), there is actually a range of some factor of 4–5 in the location of the exponential rollover, from about 60 keV up to 250 keV. I do not believe there is a "natural" temperature around 100–150 keV that always occurs. There is much broader variation in hard tail properties than is usually presumed. Furthermore, to fit the galactic black hole spectra, or the M81* spectra discussed here, what one really needs is a Compton y-parameter near ~ 1. The jet models do provide that, albeit in the regime of high coronal temperature and low optical depth, as you point out. The question then arises as to whether these high temperature/low optical depth coronae will pair-produce and cool down too much. We agree that this is an issue that needs further exploration with the jet models. An important next step in developing these models is to consider pair production. This may change the parameter regime that we consider when applying jet fits.

Acknowledgements. We are grateful to our coauthors: Herman Marshall, Claude Canizares, Alison Peck, Melanie Krips, Glen Petitpas, Rainer Schdel, Geoffrey Bower, Poonam Chandra, Alak Ray, Michael Muno, Sarah Gallagher, Seth Hornstein, & Teddy Cheung; they helped to carry out the multi-wavelength observations described in this work. We acknowledge the support of NASA Grant SV3-73016 for initial support of this work, and NASA Grant GO8-9036X for supporting attendance at this conference.

References

Baganoff F.K., Bautz M.W., Brandt W.N., et al., 2001, Nature 413, 45

Devereux N., Ford H., Tsvetanov Z., Jacoby G., 2003, AJ 125, 1226

Falcke H., Körding E., Markoff S., 2004, A&A 414, 895

Freedman W.L., Hughes S.M., Madore B.F., et al., 1994, ApJ 427

Gordon K.D., Pérez-González P.G., Misselt K.A., et al., 2004, ApJS 154, 215

Grossan B., Gorjian V., Werner M., Ressler M., 2001, ApJ 563, 687

Makishima K., Fujimoto R., Ishisaki Y., et al., 1994, PASJ 46, L77

Markoff S., Falcke H., Fender R., 2001, ApJ 372, L25

Markoff S., Nowak M., Wilms J., 2005, ApJ 635, 1203

Markoff S., Nowak M.A., Young A.J., et al., 2008, ApJ 681, 905

Murphy E.J., Braun R., Helou G., et al., 2006, ApJ 638, 157

Narayan R., Yi I., 1995, ApJ 452, 710

Nowak M.A., Wilms J., Heinz S., et al., 2005, ApJ 626, 1006

Wilms J., Nowak M., Pottschmidt K., et al., 2006, A&A 447, 245

Young A.J., Nowak M.A., Markoff S., et al., 2007, ApJ 669, 830